

Exploring the Spectrum Power Fractal Scaling Parameters by Hurst Range Increment - Second Order Moment Generation Techniques

¹Muhammad Ilyas, ²Shaheen Abbas, ¹Kamran Malik

¹Department of Mathematics Government College University Hyderabad, Sindh. Pakistan

²Laboratory of Applied Mathematics and Data Analysis (LAMDA, Al-Khwarazm DIUI Unit) Mathematical Sciences Research Centre, Federal Urdu University of Arts, Sciences and Technology, Karachi, Pakistan

*Correspondance: dr.m.ilyas@gcu.edu.pk, +923128411717

Citation | Ilyas. M, Abbas. S, Malik. K, “Exploring the Spectrum Power Fractal Scaling Parameters by Hurst Range Increment - Second Order Moment Generation Techniques”, IJIST, Vol. 6, No. 3, pp. 1328-1338, Aug 2024

Received | Aug 03, 2024 **Revised** | Aug 23, 2024 **Accepted** | Aug 25, 2024 **Published** | Aug 26, 2024.

Spectral power analysis was employed to assess the Fractal Dimension (FD) and explore fractal scaling using Hurst increment ranges and second-order moment relations in the context of urban population trends. This research aimed to scrutinize population trends in Karachi over both uneven periods (1729 to 1946) and even periods (1951 to 2020) using non-parametric Mann-Kendall tests and Hurst error accuracy testing. The primary focus was on analyzing spectrum power fractal scaling through Hurst exponent ranges and second-order moment generation. The FD results indicated irregular (1.371) and regular (1.058) intervals within the inequality range of $1 < D < 1.5$. The log-population trend cumulatively increased from 3.0 in 1729 to 5.72 in 1946, and from 6.05 in 1951 to 7.36 in 2020, suggesting that the fractal dimension is more appropriately fitted for total regular intervals. The second-order and range exponents were H_{2ndM} (0.60 ± 0.09) and H-Range (0.83 ± 0.05) for the uneven period (1729 to 1946), and H_{2ndM} (0.85 ± 0.06) and H-Range (0.93 ± 0.02) for the even period (1951 to 2020). The study's results demonstrate that the range increment method is suitable and consistent across both long and short intervals. For regular intervals, the Hurst exponents show a linear relationship, indicating stability in the population trend analysis.

Keywords: Fractal Dimension (FD), Mann-Kendall test, Spectrum power fractal scaling, Hurst Range increment (H_{Range}), Hurst Second Order Moment Generation (H_{2ndM}).



Introduction:

The analysis of urban morphologies relies on urban models that simulate and reflect the characteristics of urban spatial patterns. These models are valuable for understanding the complexities of urban growth and spatial distribution [1] [2]. Trends in data are crucial for addressing real-world problems, typically defined as average changes per unit [3] [4]. In ecological studies, trend analysis of time series data is essential, particularly when data intervals range from small to large values over time, as seen in population dynamics [5] [6]. The Mann-Kendall test is widely used for investigating trends in urban phenomena [7] [8] [9]. The assessment of fractal dimensions in time series data has garnered significant attention due to its implications for understanding complex, self-similar structures across various fields. This study focuses on evaluating the dispersion analysis method for estimating the fractal dimension of one-dimensional time series. This method is particularly relevant for signals with values measured at even time intervals, providing insights into the underlying structural properties of the data [5].

Fractal dimensions, denoted as D , characterize the roughness or complexity of a signal, where H is the Hurst coefficient related to the fractal dimension by $H = 2 - D$ [10]. The Hurst coefficient H quantifies the degree of autocorrelation or smoothness in a signal, with H values approaching 0 indicating maximal roughness or anticorrelation, and values near 1 signifying smoother, positively correlated signals. For one-dimensional series, the fractal dimension D falls within the range $1 < D < 2$, where a higher D reflects increased complexity [11].

Dispersion analysis, introduced in 1988, has become a pivotal technique for assessing fractal characteristics across various applications, including regional flow distributions in biological systems like the heart, lung, and kidney [12]. The method involves estimating the variance of a signal at multiple resolution levels and plotting the logarithm of this variance against the logarithm of the resolution size. For fractal signals, this plot yields a straight line with a slope of $1 - D$, providing a straightforward approach to quantifying the degree of heterogeneity in the signal [13].

This study builds upon the foundational work of dispersion analysis by applying it to a variety of one-dimensional time series signals, including those relevant to biological and environmental contexts. The robustness of dispersion analysis compared to traditional methods such as the Hurst rescaled range analysis will be evaluated [14]. The latter method, while well-established, faces limitations, particularly in estimating fractal dimensions from shorter data sets due to its sensitivity to local correlations and nonstationary signals [15]. This research provides an assessment of fractal theory applied to urban studies, focusing on cities like Karachi, which exhibit fractal characteristics. Urban morphologies are often fractal, displaying self-affinity and self-similarity [16] [17]. This study calculates the fractal behavior of Karachi over different periods using fractal techniques related to the fractal dimension. The current methodology involves manipulating the Hurst exponent within the fractal approach [18] [19]. The Hurst exponent is a modern method for analyzing fractal scales, used to evaluate the memory characteristics of data series through fractal scaling [20].

Objectives of Study:

This research aims to explore the relationship between urban population dynamics and fractal dimensions, considering Karachi as a fractal city. The study involves computing urban population data intervals to estimate fractal dimensions, applying spectral power fractal scaling, and comparing Hurst exponent estimates from Range Increment and Second Order Moment techniques. Error-correction formulas for fractal dimension and Hurst exponent estimation, along with the Fractal-Hurst relationship of urban population data, are also discussed.

Data and Methodology:

The research examines Karachi's population dynamics across two distinct time intervals: an uneven period (1729-1946) and an even period (1951-2020). The data sources include (i) historical gazetteer records from 1729 to 1946 and (ii) annual population data from 1951 to 2020 provided by the Pakistan Bureau of Statistics. Fractal features of population evolution were analyzed by calculating the Hurst exponent (H) for these intervals. Power spectrum analysis was employed to identify fractal scaling, and comparisons between Range Increment and Second Order Moment Generation techniques were made to validate the persistence and anti-persistence observed in population fluctuations. Additionally, the study addresses errors associated with Hurst exponent calculations.

Computational Models and Simulations:

The research utilized computational models to simulate population growth and fractal dynamics. These simulations were run on a distributed computing platform to handle the complex calculations and large data volumes. Python's scikit-learn library was used for model development and performance evaluation, providing insights into the persistence and anti-persistence observed in population data.

Spectrum Power Fractal Dimension:

The fractal dimension D is the state

$$B(p, r) = \{x: dist(x, p) < r\} \tag{1}$$

Where, B (p, r) is Hausdorff dimension by the p is a center point and r is the radius of particular phenomena, the dist (x, p) is the group between the one selected point x and other point p. Hypothetical x remains a subset of R_n bounded in N(r) showing of range compact, otherwise equal to r. Once r is gradients to 0, N(r) is increases is 1/r deliberating to power(1,2),

$$D = \lim_{r \rightarrow 0} \left(- \frac{\log N(r)}{\log r} \right) \tag{2}$$

Where, D is Hausdorff dimension, the log r → ∞ the symbol - is obligatory that D is positive (1,4,7).

$$N(r) \approx const r^D \tag{3}$$

N(r) is increases of asymptotically by r^D.

$$D = \frac{\log \left[\frac{N_n}{N_{n-1}} \right]}{\log \left[\frac{r_n}{r_{n-1}} \right]} \tag{4}$$

where N_n to direct a curve by a scale r_n (1,2).

Also, self-affinity is specified as numerous power laws e.g. Hurst exponent **H** , H = 2 – D .The fractal dimension D is specific by Hausdorff and found by (9,10), is expressed

$$H_d(s) = \begin{cases} \infty & 0 < d < D \\ 0 & D < d < \infty \\ h & d = D \end{cases} \tag{5}$$

If d = D, h is a finite value, numerically describes the size of data intervals.

Hurst Exponent by Fractal Parameter Scaling

Hurst Exponent is mostly used to valuation of the memory of any data series, Supposed that a stochastic data series is measured x(t) is a fractal nature previously x(b t) is parallel to b^H x(t), Superscript H is designed the Hurst Exponent, the stochastic data series are computed

$$0 < 0.5 < 1, \text{ if } 0 < H < 0.5 \text{ and } 0.5 < H < 1 \tag{6}$$

Suppose that {y(t)} is disreputable as a random or Brownian process on the continuous time series, which is considered a persistent or anti-persistent series. uncertainty for a time step Δt is incensement is as related

$$\Delta y(t) = y(t + \Delta t) - y(t) \tag{7}$$

As comparative variance Δt , the successive increments $\Delta y(t)$, $y(t + \Delta t)$ are not correlated. The correlation ρ , autonomous of time t , separated in

$$2^{2H} = 2 + 2\rho \left(-\frac{1}{2} < \rho < 1\right) \tag{8}$$

Indecision, $\{y(t)\}$ is a fractal procedure in Hurst exponent H , earlier, $\forall c > 0$,

$$y_c = \left(\frac{1}{c^H}\right) y(ct) \tag{9}$$

This is a further fractal form of comparable statistical properties

Hurst Exponent Range Increment-Second Order Moment Generation:

The Hurst exponent (H) is a crucial metric used to assess the persistence or anti-persistence in data series, particularly within the framework of fractal analysis. The Range Increment method evaluates the size of variation in the data by analyzing the range of increments over time, providing insights into long-term dependence and self-affinity [9]. In contrast, the Second Order Moment Generation method calculates the exponent by measuring the scaling behavior of the second-order statistical moments of the data. By employing both techniques, the authors ensure a comprehensive and robust evaluation of the Hurst exponent, enhancing the accuracy of identifying the fractal properties and temporal dynamics of population deviations. The comparison of results from these methods further confirms the presence of persistence or anti-persistence in population trends. In the stochastic process of fractal any *time* Δt , the compatible Δy is an explanation value 0 and equals

$$E(\Delta y^2) = c\Delta t^{2H} \tag{10}$$

The average of Δy^2 is an impartial estimator of $E(\Delta y^2)$ $\Delta x^2 = \Delta t^{2H}$ of $E(\Delta y^2)$ also $\Delta x^2 = \Delta t^{2H}$. Δx^2 are the instant and Δt is a period stage comprising the three-dimensional increments (1,2).

$$E(\Delta y(\Delta t^{2H})) = c\Delta t^{2H} \Rightarrow \ln E(\Delta y\Delta y(\Delta t^2)) = \ln c + 2H\ln\Delta t \tag{11}$$

$$E(\Delta y(2\Delta t^2)) = c(2\Delta t^{2H}) \Rightarrow \ln E(\Delta y(2\Delta t^2)) = \ln c + 2H\ln 2\Delta t \tag{12}$$

By Deducing the two equations (11 and 12)

$$\begin{aligned} \ln E[y(t + 2\Delta t) - y(t)]^2 - \ln E[y(t + \Delta t) - y(t)]^2 &= 2H(\ln 2\Delta t - \ln\Delta t) \\ &= 2H(\ln 2\Delta t / \Delta t) = 2H\ln 2 \end{aligned} \tag{13}$$

Consequently,

$$H = \frac{1}{(2\ln 2)} \{ \ln E[y(t + 2\Delta t) - y(t)]^2 - \ln E[y(t + \Delta t) - y(t)]^2 \} \tag{14}$$

Supposedly, the Hurst exponent is independent of the time step is determined, by the resolve of the form (14) is initiated to trial fractal molded. Hurst exponent could be computed from the coefficient correlation between the successive increments, by ($2^{2H} = 2 + 2\rho \left(-\frac{1}{2} < \rho < 1\right)$). Underneath the $e \Delta t$ has a predictable value of 0, by obtaining ρ resolved by

$$\rho = \frac{E[y(t+2\Delta t)-y(t+\Delta t)][y(t+\Delta t)-y(t)]}{\sqrt{E([y(t+2\Delta t)-y(t+\Delta t)]^2)E([y(t+\Delta t)-y(t)]^2)}} \tag{15}$$

The prospect of the equation is the unbiased estimator for the expectation.

$$\left\{ \begin{aligned} &[y(t + 2\Delta t) - y(t + \Delta t)][y(t + \Delta t) - y(t)] \\ &[y(t + 2\Delta t) - y(t + \Delta t)]^2 \\ &[y(t + 2\Delta t) - y(t)]^2 \end{aligned} \right. \tag{16}$$

Hurst exponent is found

$$2^{2H} = 2 + 2\rho \text{ which is } H = \ln(2 + 2\rho) / \ln 4 \tag{17}$$

The range increment is the variance between the highest and lowest values of $y(t)$. let's the $R(\Delta t)$ is the average range in all intervals and Δt is in the fractal process $\{y(t)\}$, In the equation below,

$$y^c = \left(\frac{1}{c^H}\right) yct \tag{18}$$

Where, $\{y(t)\}$ and $\{y_c(t)\}$ are the alike expected series (1,2). It is that the range procedure $\{y_c(t)\}$, Δt is $\frac{1}{c^H}$ time the range is $\{y(t)\}$ is time period $\Delta t/c$. Substituting $\Delta t/c$ by Δt , $R(\Delta t)$ is the average range in the time interval Δt

$$R(\Delta t) = C\Delta t^H \tag{19}$$

Application of Spectrum Fractal Scaling:

Supposedly, an urban city concerning fractal cities, which is detected that the central distance r reliant on the population size p , $r \propto p^d$

$$r(p) = kpd \tag{20}$$

$$\log(r) = \log(k) + d\log p \tag{21}$$

So, d is the slope of abscissa the logarithm of the step size, and of ordinate the logarithm The power laws is

$$y = f(x) = \text{const } x^c \tag{22}$$

exponent c . scale invariance involves

$$f(ax) = bf(x) \tag{23}$$

$$f(x) = \text{const } x^c \tag{24}$$

Where

$$c = \log b / \log a$$

$$\log y = \log(\text{const}) + c \log x \tag{25}$$

Non-Parametric test:

The Mann-Kendall test reflects n data values along with T_j and T_i is the subgroup of data here, $i = 1, 2, 3, \dots, n-1$ and $j = i+1, i+2, \dots, n$.

$$S = \sum_{i=1}^{n-1} \sum_{j=i+1}^n \text{sign}(T_j - T_i) \tag{26}$$

$$\text{sign}(T_j - T_i) = \begin{cases} 1 & \text{if } T_j - T_i > 0 \\ 0 & \text{if } T_j - T_i = 0 \\ -1 & \text{if } T_j - T_i < 0 \end{cases} \tag{27}$$

Where T_j and T_i are the first and second data values are assessed as an order of time series. The Statistic Z_s test is obtained as express

$$Z_s = \begin{cases} \frac{s-1}{\sigma} & \text{for } s > 0 \\ 0 & \text{for } s = 0 \\ \frac{s+1}{\sigma} & \text{for } s < 0 \end{cases} \tag{28}$$

The Z_s test is computed for the consequence of the trend. The Z_s stands the test of null of hypothesis, H_0 , the coefficient value of $|Z_s| < |Z_{\alpha/2}|$. The following algorithm was utilized to perform nonparametric test.

```
import pandas as pd
from scipy.stats import mannwhitneyu, kruskal, wilcoxon, friedmanchisquare,
chi2_contingency

# Load data
data = pd.read_csv('your_data.csv')

# Example 1: Mann-Whitney U Test
group1 = data[data['Group'] == 'A']['Value']
```

```

group2 = data[data['Group'] == 'B']['Value']
stat, p_value = mannwhitneyu(group1, group2)
print(f'Mann-Whitney U statistic: {stat}, P-value: {p_value}')

# Example 2: Kruskal-Wallis H Test
group1 = data[data['Group'] == 'A']['Value']
group2 = data[data['Group'] == 'B']['Value']
group3 = data[data['Group'] == 'C']['Value']
stat, p_value = kruskal(group1, group2, group3)
print(f'Kruskal-Wallis H statistic: {stat}, P-value: {p_value}')

# Example 3: Wilcoxon Signed-Rank Test
before = data[data['Time'] == 'Before']['Value']
after = data[data['Time'] == 'After']['Value']
stat, p_value = wilcoxon(before, after)
print(f'Wilcoxon Signed-Rank statistic: {stat}, P-value: {p_value}')

# Example 4: Friedman Test
group1 = data[data['Treatment'] == 'X']['Value']
group2 = data[data['Treatment'] == 'Y']['Value']
group3 = data[data['Treatment'] == 'Z']['Value']
stat, p_value = friedmanchisquare(group1, group2, group3)
print(f'Friedman statistic: {stat}, P-value: {p_value}')

# Example 5: Chi-Square Test for Independence
contingency_table = pd.crosstab(data['Category1'], data['Category2'])
stat, p_value, dof, expected = chi2_contingency(contingency_table)
print(f'Chi-Square statistic: {stat}, P-value: {p_value}, Degrees of freedom: {dof}')
print(f'Expected frequencies: \n{expected}')

```

Accuracy of Error:

The power spectrum $S(\omega)$ frequently is oppressed by the execution of a Fourier transform on the series paths the power law recital over a significant frequency scale [3] as definite by

$$S \propto \omega^{-\beta} \quad (29)$$

$$H = \frac{\beta-1}{2} \quad (30)$$

Fractal scaling is exposed to arise after the scaling is projected by manipulating the extent of the data or else in assessing scaling in the power spectrum.

Results and Discussion:

In this research, population data for Karachi was analyzed across two distinct time intervals: 1729-1946 and 1951-2020. These intervals were categorized into historical and recent periods, with data series examined through spectral power fractal scaling using the Hurst exponent, Second Order Moment, and Range Increment methods. Error calculations for the Hurst exponent and trend analysis using the Mann-Kendall statistic validated the fractal scaling. The integration of computational tools and models significantly enhanced the accuracy and reliability of the fractal and statistical analyses. The use of high-performance computing and advanced data processing techniques allowed for precise calculations of the Hurst exponent and fractal dimensions.

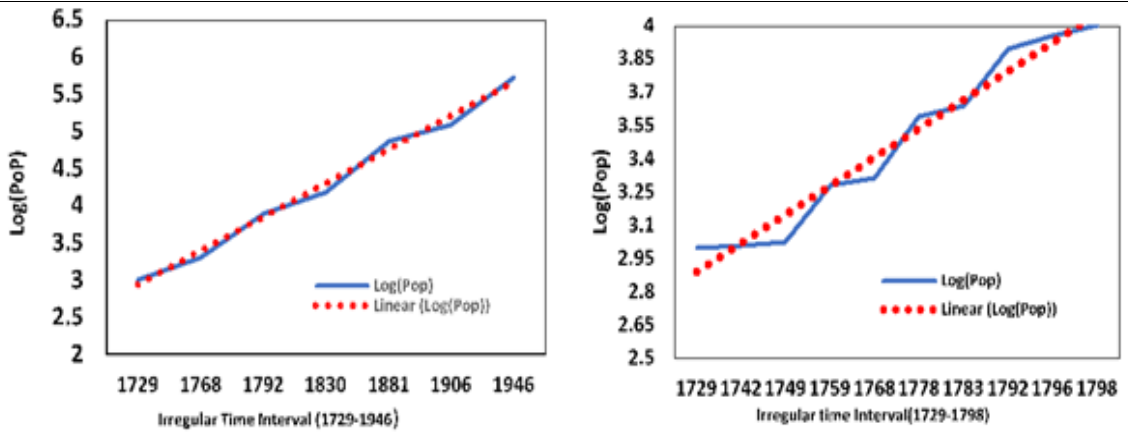


Figure 1. Linear Trend Irregular Population interval from 1729-1946 and 1729-1798

Table 1. shows that the non-parametric Kendall's test applied to the irregular data (1729-1946) and the regular data (1951-2020) reveals that the Kendall coefficient $|Z_s|$ is significantly higher than $|Z_\alpha|$. This indicates a stronger trend in the even intervals compared to the uneven intervals, as illustrated in Figures 1 to 6. The trend in the even interval shows a consistent increase compared to earlier periods. Additionally, with S statistic and $p < \alpha$ (0.05), the null hypothesis (H_0) is rejected, confirming a significant trend in the data series.

Table 1. Non-parametric analysis for logarithm population data series 1729 to 2020.

Mann-Kendall statistic	1729-1798	1810-1897	1901-1946	1729-1946	1951-2020
<i>Kendall's tau</i>	0.978	0.744	1.000	0.966	0.999
<i>Kendall statistic (S)</i>	89.000	58.000	45.000	643.000	1889.0
<i>Var(S)</i>	1232.00	1236.00	5676.23	5845.000	27104.3
<i>Alpha</i>	0.05	0.05	0.05	0.05	0.05
<i>p-value (Two-tailed)</i>	<.001	<.001	<.001	<.001	<.001
$ z_s $	4.443	4.165	5.486	3.997	13.622
$ z_{\alpha/2} $	1.960	1.960	1.960	1.960	1.960
$ t_s $	4.443	4.165	5.486	3.997	13.622
$ t_{\alpha/2} $	2.160	2.179	2.262	2.028	2.000

Further analysis explored the relationship between population and fractal dimension. For the uneven interval (1729-1946), the log-population (p) versus fractal dimension (D) is described by $\text{Log(P)}_{ir} = 0.8647D + 3.1933$. For the even interval (1951-2020), it is $\text{Log(P)}_r = 0.2035D + 6.1014$. The coefficient of determination indicates a strong positive correlation between the log-linear functions of population and fractal dimensions, as shown in Table 2 (a-b) and Figure 6.

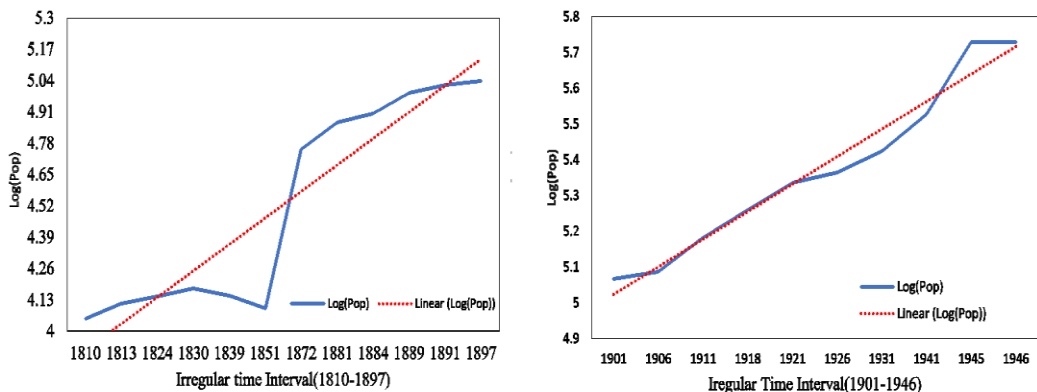


Figure 2. Linear Trend Irregular Population interval from 1810-1897 and 1901-1946

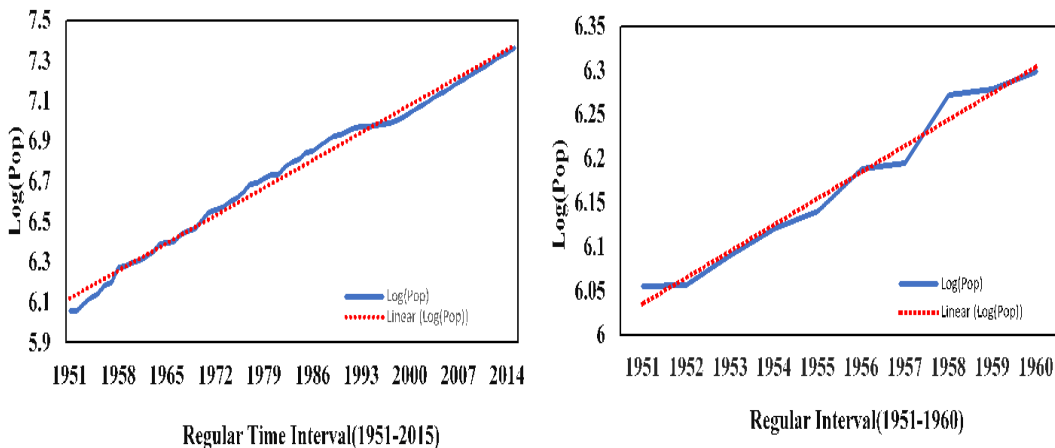


Figure 3. Linear Trend Regular Population interval from 1951-2020 and 1951-1960

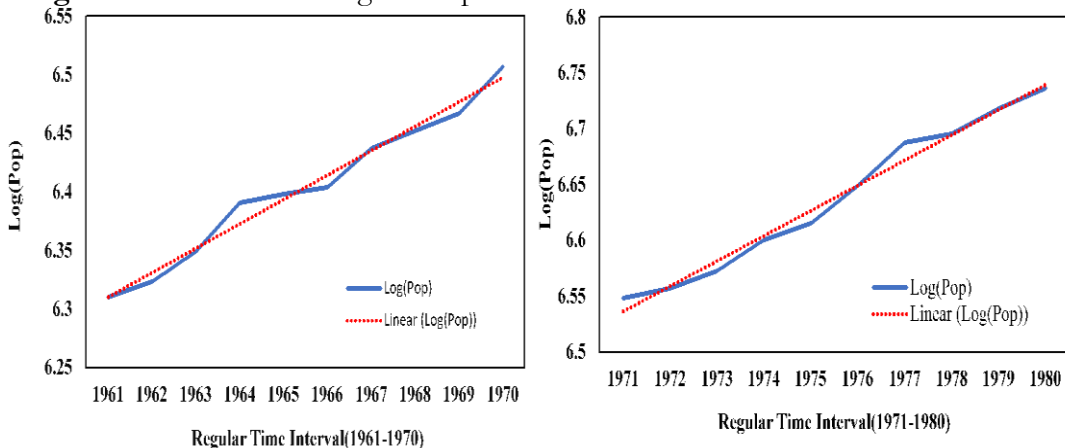


Figure 4. Linear Trend Regular Population interval from 1961 to 1970 and 1971 to 1980..

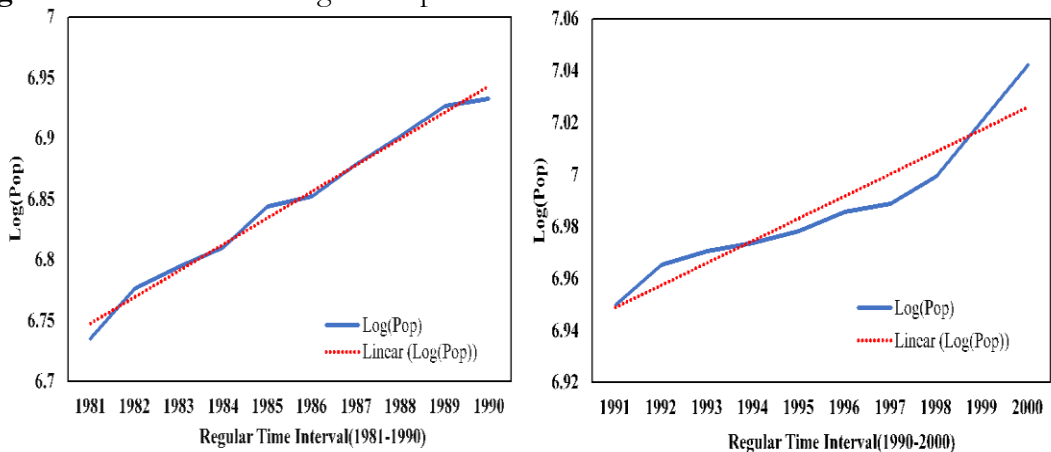


Figure 5. Linear Trend Regular Population interval from 1981-1990 and 1991-2000.

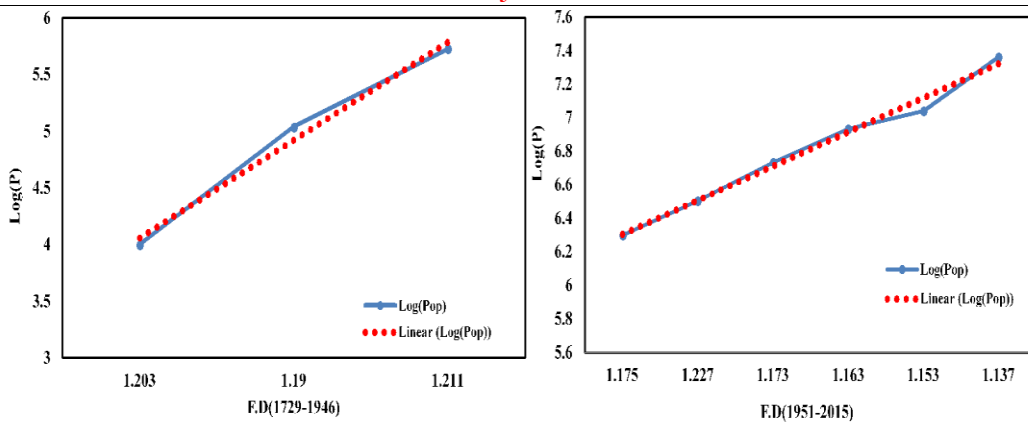


Figure 6. Fractal Dimension versus log (pop) functions for Total Irregular (1729-1946) and Regular Intervals (1951-2020).

Table 2. (a) Fractal Dimension and Hurst Exponents for Irregular and Regular Population intervals

Date Interval	Hurst Exponent	Fractal Dimension
1729-1946	0.629	1.371
1729-1798	0.797	1.203
1810-1897	0.81	1.190
1901-1946	0.789	1.211
1951-2015	0.942	1.058
1951-1960	0.825	1.175
1961-1970	0.773	1.227
1971-1980	0.827	1.173
1981-1990	0.837	1.163
1991-2000	0.847	1.153
2001-2020	0.863	1.137

Table 2. (b) The Logarithm population along Fractal Dimension and Hurst Exponents

Time Interval	F. D	Log(p)	R2	Log(p) estimated	Log(p) Actual	Hurst Exponent
1729-1946	1.371	$y = 0.8647p + 3.1933$	0.9867	4.378804	5.72835	0.629
1951-2020	1.058	$y = 0.2035p + 6.1014$	0.9884	6.316703	7.033741	0.942

Table 2. (a-b) highlights that the log population increased from 3.0 in 1729 to 5.73 in 1946 and from 6.06 in 1951 to 7.36 in 2020. Conversely, the Fractal Dimension (FD) varied from 1.371 (1729-1946) to 1.058 (1951-2020), demonstrating that both irregular and regular population data series fall within the inequality range $1 < D < 1.5$. This correlation underscores that fractal dimensions are a reasonable measure for even intervals. The Hurst exponents, calculated using the Range Increment and Second Order Moment methods, show values of $H_{2ndM} = 0.60$ and $H_{Range} = 0.83$ for the irregular period (1729-1946) and $H_{2ndM} = 0.85$ and $H_{Range} = 0.99$ for the regular period (1951-2020), as detailed in Table 3.

Table 3. Hurst Exponent Obtain by H_{RangeM} and H_{2ndM} from 1729 to 2020

Irregular interval	Second Moment Growth (H_{2ndM})	Range increment(H_{Range})
1729 to 1798	0.59 ± 0.06	0.72 ± 0.02
1810 to 1898	0.51 ± 0.04	0.66 ± 0.03
1901 to 1946	0.56 ± 0.07	0.79 ± 0.03
1729 to 1946	0.60 ± 0.09	0.83 ± 0.05

Regular Interval	Second Moment Growth (H _{2ndm})	Range Increment (H _{Range})
1951 to 1960	0.56 ± 0.07	0.69 ± 0.03
1961 to 1970	0.58 ± 0.02	0.60 ± 0.03
1971 to 1980	0.66 ± 0.02	0.90 ± 0.06
1981 to 1990	0.68 ± 0.02	0.82 ± 0.03
1991 to 2000	0.72 ± 0.02	0.82 ± 0.05
2000 to 2020	0.82 ± 0.01	0.87 ± 0.01
1951 to 2020	0.85 ± 0.06	0.99 ± 0.02

Both irregular and regular data series show Hurst exponents (H) > 0.5, indicating a positive correlation with fractal dimensions (Table 2). The Hurst exponent values between 0.5 and 1 suggest a confident and increasing trend. This research confirms that spectral fractal dimensions inversely correlate with the Hurst exponent, with an increasing fractal dimension corresponding to a decreasing Hurst exponent. The data interval demonstrates a close-fitting persistence in the Hurst exponent, reflecting an interactive gradient of trend fitting for regular data series.

Conclusion:

This study examines population inequality in Karachi using spectrum power fractal scaling through the Second Moment and Range Increment methods to analyze the Hurst Exponent. The analysis of data intervals from 1729 to 1946 and 1951 to 2020 revealed that recent decades exhibit a smoother and more pronounced increase compared to earlier periods. The findings confirm a strong positive correlation and persistence in the population data. Log-linear functions versus fractal dimensions support the conclusion that Hurst Exponent values exceeding 0.5 indicate persistent data series. Additionally, the Range Increment method consistently produces higher values than the Second Moment technique across both irregular and regular datasets. Overall, the research provides valuable insights into the dynamics of population evolution and the patterns of inequality in Karachi over several centuries.

References:

- [1] H. E. Hurst, "Long-Term Storage Capacity of Reservoirs," *Trans. Am. Soc. Civ. Eng.*, vol. 116, no. 1, pp. 770–799, Jan. 1951, doi: 10.1061/TACEAT.0006518.
- [2] P. J. Taylor, "Quantitative methods in geography: an introduction to spatial analysis," p. 386, 25431BC.
- [3] Asma Zaffar, S. Abbas, and M. R. K. Ansari, "A Study of Largest Active Region AR12192 of 24th Solar Cycle Using Fractal Dimensions and Mathematical Morphology," *Sol. Syst. Res.*, vol. 54, no. 4, pp. 353–359, Jul. 2020, doi: 10.1134/S0038094620040012/METRICS.
- [4] S. Abbas and M. Ilyas, "Assessing the impact of EI Niño southern oscillation index and land surface temperature fluctuations on dengue fever outbreaks using ARIMAX(p)-PARX(p)-NBARX(p) models," *Arab. J. Geosci.*, vol. 11, no. 24, pp. 1–12, Dec. 2018, doi: 10.1007/S12517-018-4119-9/METRICS.
- [5] S. Katsev and I. L'Heureux, "Are Hurst exponents estimated from short or irregular time series meaningful?," *Comput. Geosci.*, vol. 29, no. 9, pp. 1085–1089, Nov. 2003, doi: 10.1016/S0098-3004(03)00105-5.
- [6] M. F. . Barnsley and H. Rising, *Fractals everywhere*. Academic Press Professional, 1993. Accessed: Sep. 01, 2024. [Online]. Available: <http://www.sciencedirect.com:5070/book/9780120790616/fractals-everywhere>
- [7] D. Hassan, S. Abbas, and & M. R. K. Ansari, "COMPARATIVE STUDY OF SOLAR FLARE NORTH-SOUTH HEMISPHERIC AND K-INDEX GEOMAGNETIC ACTIVITY TIME SERIES DATA USING FRACTAL DIMENSION," *Gomal Univ. J. Res.*, vol. 33, no. 1, pp. 72–79, Jun. 2017, Accessed: Sep. 01, 2024. [Online]. Available:

- <http://www.gujr.com.pk/index.php/GUJR/article/view/84>
- [8] “(PDF) Fractal analysis of time series and distribution properties of Hurst exponent.” Accessed: Sep. 01, 2024. [Online]. Available: https://www.researchgate.net/publication/281092858_Fractal_analysis_of_time_series_and_distribution_properties_of_Hurst_exponent
- [9] M. J. Kirkby, “The fractal geometry of nature. Benoit B. Mandelbrot. W. H. Freeman and co., San Francisco, 1982. No. of pages: 460. Price: £22.75 (hardback),” *Earth Surf. Process. Landforms*, vol. 8, no. 4, pp. 406–406, Jul. 1983, doi: 10.1002/ESP.3290080415.
- [10] K. Pollok, B. Jamtveit, and A. Putnis, “Analytical transmission electron microscopy of oscillatory zoned grandite garnets,” *Contrib. to Mineral. Petrol.*, vol. 141, no. 3, pp. 358–366, 2001, doi: 10.1007/S004100100248.
- [11] G. L. Trigg, “Mathematical Tools for Physicists,” *Math. Tools Phys.*, pp. 1–676, May 2006, doi: 10.1002/3527607773.
- [12] P. W. O. Hoskin, “Patterns of chaos: Fractal statistics and the oscillatory chemistry of zircon,” *Geochim. Cosmochim. Acta*, vol. 64, no. 11, pp. 1905–1923, Jun. 2000, doi: 10.1016/S0016-7037(00)00330-6.
- [13] J. B. Bassingthwaite and G. M. Raymond, “Evaluation of the Dispersional Analysis Method for Fractal Time Series,” *Ann. Biomed. Eng.*, vol. 23, no. 4, p. 491, Jul. 1995, doi: 10.1007/BF02584449.
- [14] J. Gao, Y. Cao, W. Tung, and J. Hu, “Basics of Fractal Geometry,” *Multiscale Anal. Complex Time Ser.*, pp. 69–77, Aug. 2007, doi: 10.1002/9780470191651.CH5.
- [15] R. F. Mulligan, “The multifractal character of capacity utilization over the business cycle: An application of Hurst signature analysis,” *Q. Rev. Econ. Financ.*, vol. 63, pp. 147–152, Feb. 2017, doi: 10.1016/j.qref.2016.04.016.
- [16] T. M. Tóth, “Fracture network characterization using 1D and 2D data of the Mórággy Granite body, southern Hungary,” *J. Struct. Geol.*, vol. 113, pp. 176–187, Aug. 2018, doi: 10.1016/j.jsg.2018.05.029.
- [17] M. Tarnopolski, “Correlation between the Hurst exponent and the maximal Lyapunov exponent: Examining some low-dimensional conservative maps,” *Phys. A Stat. Mech. its Appl.*, vol. 490, pp. 834–844, Jan. 2018, doi: 10.1016/j.physa.2017.08.159.
- [18] A. Mittal, S. S. Mallick, and P. W. Wypych, “An investigation into pressure fluctuations for fluidized dense-phase pneumatic transport of fine powders,” *Powder Technol.*, vol. 277, pp. 163–170, Jun. 2015, doi: 10.1016/j.powtec.2015.02.052.
- [19] K. T. Park *et al.*, “Characterization and expression of monoclonal antibody-defined molecules on resting and activated bovine $\alpha\beta$, $\gamma\delta$ T and NK cells,” *Vet. Immunol. Immunopathol.*, vol. 168, no. 1–2, pp. 118–130, Nov. 2015, doi: 10.1016/j.vetimm.2015.09.002.
- [20] C. Walck, “Hand-book on STATISTICAL DISTRIBUTIONS for experimentalists,” 1996.



Copyright © by authors and 50Sea. This work is licensed under Creative Commons Attribution 4.0 International License.